Assessment of altered brain function in patients with psychogenic non-epileptic seizures using resting-state functional MRI

M. Vardian[1,2,3*], M.A. Oghabian[1,2], M. Arbabi[4], T. Ebrahimi[1,2]

[1]Department of Medical Physics and Biomedical Engineering, School of Medicine, Tehran University of Medical Sciences, Tehran, Iran
[2]Department of Neuroimaging and Analysis, Imam Khomeini Hospital Complex, Tehran University of Medical Sciences, Tehran, Iran
[3]Medical Physics Group, School of Medicine, Fasa University of Medical Sciences, Fasa, Iran
[4]Department of Psychiatry, Brain & Spinal Cord Injury Research Center, Psychosomatic Medicine Research Center, Tehran University of Medical Sciences, Tehran, Iran

ABSTRACT

► *Original article*

Background: Psychogenic non-epileptic seizure (PNES) is a disease characterized by the alternations in the brain network. The current study aimed to assess the global and local brain network changes in various brain regions for the patients with PNES using functional magnetic resonance imaging (fMRI). **Materials and Methods**: The resting-state fMRI (rs-fMRI) data of 32 adults (ranged from 22-61 years; mean: 33.1±7.2), including 16 healthy controls and 16 PNES patients, were obtained. Several standard global network parameters, including small-worldness, average clustering coefficient, characteristic path length, and global efficiency, were investigated. Nodal characteristics, such as the degree of centrality (DC), betweenness centrality (BC), nodal efficiency (NF), nodal local efficiency (NLF), nodal clustering coefficient (NCC), and shortest route, were also determined independently for each node (region) to represent local changes in the brain network. The local and global parameters' values were compared between healthy individuals and PNES patients using Mann-Whitney statistical test. **Results**: There was no significant difference among the global parameter values obtained from PNES patients and healthy individuals (P>0.05). However, many local brain network parameters showed statistically significant differences in the functional connectivity networks (P<0.05), including attentional, sensorimotor, default mode, executive control networks, and subcortical area. **Conclusion**: Although global brain network parameters calculated from fMRI images were similar between healthy and PNES participants, many local brain network parameters showed statistically significant differences. Our findings support PNES patients' hypoactivity in the regions associated with awareness and motor control as well as their hyperactivity in the areas associated with emotion and motion control.

INTRODUCTION

It is estimated that the human brain has about 100 billion neurons connected by 100 trillion synapses [1]. Therefore, evaluating and exploring the human brain and detecting its neural mechanisms is a complex and challenging scientific issue [1,2]. It has been reported that the simple or complex functions in the brain are not performed independently by specific neurons or brain areas but by a cluster of neurons in one or several brain network regions [3,4]. The brain can be modeled as a complex network with high power and information transfer efficiency [5].

Various psychiatric and neurological diseases are associated with brain structural and/or functional changes. Different neuroimaging techniques can be used as a tool for physicians and researchers to study these changes [6,7]. Magnetic resonance imaging (MRI) methods include structural MRI and functional MRI (fMRI), such as resting-state functional MRI (rs-fMRI) are important neuroimaging techniques for assessing brain changes. Furthermore, network-based analysis can be widely used as a quantitative method to determine the brain's structural and functional changes [8,9].

Psychogenic non-epileptic seizures (PNES) are a set of motor and emotional changes. The disease has an experience similar to epileptic seizures for a patient but has no additional electrophysiological relationship to the brain [10]. The diagnosis of psychogenic PNES includes clinical evaluation, neurology symptom assessment, and visual electroencephalography (vEEG). The average age of PNES's first diagnosis is approximately 23 years in

both genders [11]. The incidence of PNES is estimated at 1.4 to 4.9 per 100,000 people, annually, women have a three times higher risk [12]. There is strong evidence that people with PNES have higher anxiety, depression, and personality disorders than those with epilepsy. In addition, deficits in cognition and emotional processing are common features of PNES patients. On the other hand, PNES has motor, sensory, autonomic, cognitive, and emotional components without understandable EEG symptoms [13,14].

fMRI studies have shown that the resting-state functional connectivity between emotion regulation and motor control areas is different in PNES patients with healthy individuals [15-17]. PNES creates an incorrect neural connection between areas of the brain which can affect emotional executive control and leads to altered motor functions [15-17].

Several studies report brain network changes in PNES patients using fMRI techniques [18-21]. For instance, Allendorfer *et al.* [19] investigated the response to psychological stress in brain areas involved in emotional-motor-executive control in PNES patients with fMRI. In their study, 12 PNES patients and 12 healthy controls underwent stress tasks and rs-fMRI. Imaging results showed lower activity in the left/right amygdala and left hippocampus in PNES patients compared to the control group. PNES patients also had a stronger resting functional connectivity between the right amygdala, the left precentral gyrus, and the inferior/middle frontal gyrus. Van der Krujis *et al.* [21] estimated the changes in the prefrontal cortex, frontoparietal, and sensorimotor brain network areas using independent component analysis on rs-fMRI data. They demonstrated that patients with higher dissociation scores have a lower cognitive function in several regions of frontoparietal, executive control, and sensorimotor networks. Ding *et al.* [20] studied changes in functional brain connectivity in 18 PNES patients and 20 healthy individuals. They found that functional connectivity density differed in the frontal cortex of PNES patients, sensorimotor cortex, cingulate gyrus, insula, and occipital cortex.

All the previous studies reported that PNES patients undergoing fMRI had altered connectivity density, dissociation scores, and cognitive and motor functions [18-21]. However, they did not evaluate both the global and local (nodal) network parameters obtained from fMRI for PNES patients. In the current study, we aimed to assess the aforementioned network parameters obtained from rs-fMRI, compared between PNES patients and healthy individuals.

MATERIALS AND METHODS

This retrospective single-center study was approved in March 2020 by the ethical committee of Tehran University of Medical Sciences (Tehran, Iran) with the registration number of "IR.TUMS.MEDICINE.REC.1398.496".

The rs-fMRI data have been collected by a 3-T (Siemens, Erlangen, Germany) system with a 12ch head-coil. The data of 32 adults with the age range of 22-61 years (mean: 33.1 years, standard deviation: 7.2 years), including 16 healthy controls (9 women and 7 men) and 16 PNES patients (10 women and 6 men) were obtained and analyzed. Written informed consent was obtained from all participants, and they were informed that the study protocol had no invasive procedure.

The participants were asked to keep their eyes open during the fMRI. T1-weighted anatomical images were obtained with a repetition time (TR): 250 msec, time of echo (TE): 4 msec, matrix size: 128×128 pixels, and voxel dimensions: 2×2×1 mm³ before fMRI data acquisition. The echo planar imaging (EPI) was used with the following parameters to obtain the fMRI images; TR: 2.5 sec, TE: 33 msec, FOV: 208 ×180 mm², matrix size: 104× 90 pixels, voxel dimensions: 2×2×2 mm³, and the total scan time was 360 seconds to gather 144 cross-sectional images. A sample of a T1-weighted fMRI image is shown in figure 1.
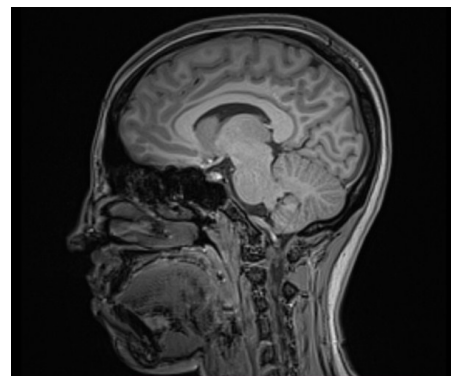

Figure 1. T1-weighted fMRI image of a 23-year-old woman with PNES.

Image preprocessing was performed using free open-source Statistical Parametric Mapping (SPM12, available at: https://www.fil.ion.ucl.ac.uk/spm) and an open-source, MATLAB-based, cross-platform package GRETNA (GRaph thEoreTical Network Analysis, available at: http://www.nitrc.org/projects/gretna/) [22]. The preprocessing steps included slice timing correction; functional realignment to exclude subjects with head motion more than 2 mm or 2 degrees; reorientation of functional and T1 images, co-registration of T1 images; segmentation; normalization with standard stereotactic (MNI) space, spatial smoothing by the Gaussian kernel with a full-width at half-maximum (FWHM) of 4 mm; extracting mean time series from white matter and CSF, and temporal band-pass filtering between 0.01 and 0.1 Hz.

Initially, the whole brain was segmented using the

automatic anatomical labeling (AAL) atlas, which divides the brain into 90 cortical and subcortical regions. The fMRI images were imported to GRETNA software. Then, adjacency matrices for each participant were determined using this software. Bivariate (z-transformed) correlation between the average signals in all voxels of a region (node) and an adjacent node was calculated for each pair of nodes. The 90×90 undirected and unweighted correlation matrix was considered as the calculation results. The total number of edges was considered fixed with a certain connection density, and the adjacency matrices were binarized regarding this assumption.

Network analysis involves calculating the brain's global and nodal network quantities in a range of connection densities between 0.050 and 0.275 with incremental steps of 0.025 to reduce the effect of threshold value selections. These values were in an appropriate range of thresholds (approximately 0.01-0.30) because many of the graph characteristics, such as small-worldness, can be obtained consecutively. The small-worldness was evaluated to be more than 1 for all participants. A free MATLAB-based toolbox, BrainNet Viewer software (available at: http://www.nitrc.org/projects/bnv/) [23], was also used to display the network parameter results. All the global and nodal parameters of the calculated brain network were calculated for all participants and compared between the PNES and healthy group members.

Global network measures

Global network parameters illustrate the brain network's functional segregation and integration. We considered several parameters for evaluating the global networks, including small-worldness (segregation and integration), average clustering coefficient (segregation), characteristic path length (integration), and global efficiency (integration).

Small-worldness demonstrates the degree of organizing the small-world, which is the optimal balance between functional integration and segregation. A small-world organization typically has sub-modules that perform specific functions (segregation), and sub-modules are interconnected for performing more advanced brain functions (high integration). The small-world calculation is determined based on the characteristic path length and clustering coefficient. The characteristic path length demonstrates the average of shortest path length values between all pairs of nodes. Global efficiency is inversely related to characteristic path length. In the case of isolated nodes, the characteristic path length is infinite; therefore, global efficiency is zero. The network criteria parameters must be compared with their corresponding values in randomly generated networks consisting of the same number of nodes, edges, and distribution degree.

Small-world networks have high clustering characteristics similar to conventional networks and short paths similar to random networks. The following three criteria (equations 1, 2 and 3) were used to specify whether a network is a small-world network:

$$\gamma = \frac{c}{c_{rand}} \tag{1}$$

$$\lambda = \frac{L}{L_{rand}} \tag{2}$$

$$\sigma = \frac{\gamma}{\lambda} \tag{3}$$

As C_{rand} and L_{rand} are the mean clustering coefficient, and the characteristic path length of a random network having the same number of nodes, edges, and similar degree distribution as the real network. γ and λ are normalized clustering coefficients and normalized path lengths, and σ is the network small-worldness index. A network with small-world characteristics must satisfy two conditions, including $\gamma \gg 1$ and $\lambda \approx 1$, and therefore $\sigma > 1$ (24–29).

Nodal network parameters

Nodal network parameters were calculated separately for each node (region), reflecting local differences between participants in PNES and healthy group members. The most widely used basic and important parameters are the degree of centrality (DC), betweenness centrality (BC), nodal efficiency (NF), nodal local efficiency (NLF), nodal clustering coefficient (NCC), and shortest path (Sh.P).

The degree of a node is the total number of edges connected to the node and is equal to the number of neighbors, which indicates the importance of the node in the network. The higher degree value represents the higher important role of the node (for example, the hub node). The clustering coefficient measures the ratio of neighbors for a node. The average clustering coefficient of three nodes in a triangle is 1, which reflects a robust clustering of these nodes. Local efficiency is the efficiency of the connection between one node and other nodes, which is equal to the inverse average of the Sh.P lengths. The small value of local efficiency reflects the long distances for information transfer between nodes. For disconnected nodes and sub-networks, the efficiency is zero. The Sh.P length of a given node measures the average distance between the node and all other nodes in the network.

Statistical analysis

The normality distribution of the assessed parameters was evaluated by Kolmogorov–Smirnov (K–S) test. The results determined that the distributions of the parameters were not normal. Therefore, the mentioned local and global parameters' values were compared between healthy individuals and PNES patients using Mann-Whitney statistical test. The SPSS software package (v. 22,

SPSS Inc., Chicago, IL, USA) was used for all of the statistical tests. P values of <0.05 were considered statistically significant.

RESULTS

Global parameters between healthy and PNES groups

Although both groups had small-worldness higher than 1 (σ> 1), the difference in the σ was not significant between the PNES patients and healthy participants (P =0.17). In addition, the values of Sh.P length, clustering coefficient, λ, and γ between the two groups were not shown a significant variation (P>0.09). Furthermore, the values of global efficiency and local efficiency did not differ significantly (P >0.20).

Nodal parameters between healthy and PNES groups

Nodal parameters were calculated separately for each node (region) and represented in table 1. These values reflect local differences in the brain network of various regions. The values of the nodal network parameters included BC, DC, NF, NLF, NCC, and Sh.P.

Table 1. Calculated nodal parameters for each node (region) with significant differences between PNES patients and healthy individuals.

AAL (90 regions)	B.C	D.C	N.E	N.L.E	N.C.C	Sh.P
FFG.R	Increase	-	Increase	-	Decrease	-
PHG.R	Decrease	Decrease	-	-	Increase	Decrease
PHG.L	-	-	-	-	-	Decrease
ORBinf.R	Increase	-	-	-	-	-
SFGdor.R	Decrease	Decrease	-	-	Increase	Decrease
SFGdor.L	Decrease	-	Decrease	-	Increase	-
HIP.R	Increase	Increase	Increase	-	-	Increase
HIP.L	-	Increase	Increase	-	-	Decrease
INS.R	Increase	Increase	Increase	Decrease	Decrease	-
INS.L	Increase	-	Increase	Decrease	Decrease	-
PUT.R	Increase	Increase	Increase	-	-	Decrease
PUT.L	-	-	Increase	-	-	Decrease
ROL.R	Increase	-	-	Decrease	Decrease	-
SOG.R	Increase	-	-	-	Decrease	-
SMG.R	Increase	Increase	Increase	-	Decrease	-
SMG.L		Increase	Increase	-	-	-
PCL.R	Decrease	-	-	-	-	-
PCL.L	Decrease	-	-	-	-	-
PCG.L	Decrease	-	-	-	Increase	-
MFG.L	Increase	-	-	-	Decrease	-
ANG.L	Increase	-	-	-	-	-
PCUN.R	-	-	Decrease	-	-	-
PCUN.L	Decrease	-		-	-	-
TPOmid.R	-	Decrease	Decrease	-	-	Decrease
TPOmid.L	-	Decrease	Decrease	Decrease	Decrease	Decrease
TPOsup.R	-	Decrease	-	-	-	-
TPOsup.L	-	Decrease	Decrease	-	-	-
STG.R	-	Decrease	-	-	-	-
HES.R	-	Decrease	Decrease	-	-	-
HES.L	-	Decrease	Decrease	-	-	-
IFGtriang.R	-	Decrease	Decrease	-	-	-
SMA.R	-	Increase	Increase	-	-	-
SMA.L	-	-	-	Increase	Increase	-
IPL.R	-	-	Increase	-	-	-
IPL.L	-	-	Increase	Increase	-	-
SPG.R	-	-	-	Increase	-	-
SPG.L	-	-	-	Increase	-	-
OLF.R	-	-	-	-	-	Decrease
OLF.L	-	-	-	Decrease	Decrease	Decrease
PreCG.L	-	-	-	Increase	-	-
AMYG.R	-	-	-	-	-	Increase
AMYG.L	-	-	-	-	-	Increase
PAL.R	-	-	-	-	-	Decrease
PAL.L	-	-	-	-	-	Decrease
THA.R	-	-	-	-	-	Decrease
THA.L	-	-	-	-	-	Decrease
CAU.R	-	-	-	-	-	Decrease
CAU.L	-	-	-	-	-	Decrease
DCG.R	-	-	-	-	-	Increase
DCG.L	-	-	-	-	-	Increase

AAL: automatic anatomical labeling, B.C: betweenness centrality, D.C: degree of centrality, N.E: nodal efficiency, N.L.E: nodal local efficiency, N.C.C: nodal clustering coefficient, Sh.P: shortest path, FFG: fusiform gyrus, PHG: para hippocampal gyrus, ORBinf: orbital part of the left inferior frontal gyrus, SFGdor: Superior frontal gyrus dorsolateral, HIP: hippocampus, INS: insula, PUT: putamen, ROL: rolandic operculum, SOG: superior occipital gyrus, SMG: supramarginal gyrus, PCL: paracentral lobule, PCG: posterior cingulate gyrus, MFG: middle frontal gyrus, ANG: angular, PCUN: posterior cingulate gyrus, TPO: temporal pole, STG: superior temporal gyrus, HES: heschl gyrus, IFG: inferior frontal gyrus, SMA: supplementary motor area, IPL: inferior parietal, SPG: superior parietal gyrus, OLF: olfactory cortex, PreCG: precental gyrus, AMYG: amygdala, PAL: pallidum, THA: thalamus, CAU: caudate nucleus, and DCG: paracingulate gyri.

Betweenness centrality (BC)

The BC values determined significant differences (P <0.05) among the PNES patients and the healthy control group in various brain regions, including the fusiform gyrus, para hippocampal gyrus, inferior frontal gyrus-orbital part, hippocampus, insula, lenticular nucleus-putamen, rolandic operculum, superior occipital gyrus, supramarginal gyrus, and paracentral lobule in the right hemisphere, and insula, posterior cingulate gyrus, middle frontal gyrus, angular gyrus, precuneus, and paracentral lobule in the left hemisphere. Figure 2 shows the mean BC values for healthy participants and PNES patients in various brain network regions.
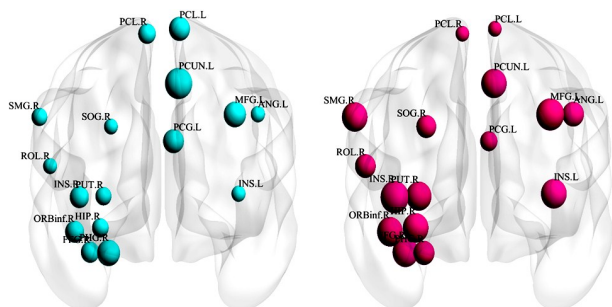

Figure 2. Mean values of betweenness centrality for healthy participants (left) and PNES patients (right) in various brain network regions. PCL: paracentral lobule, PCUN: posterior cingulate gyrus, INS: insula, MFG: middle frontal gyrus, SOG: superior occipital gyrus, PUT: putamen, ORBinf: orbital part of the left inferior frontal gyrus, SMG: supramarginal gyrus, PCG: posterior cingulate gyrus, HIP: hippocampus, ANG: angular, PHG: para hippocampal gyrus, and FFG: fusiform gyrus.

Degree of centrality (DC)

The results related to DC among PNES patients and healthy individuals showed significant differences (P<0.05) in various regions, including temporal pole-middle temporal gyrus, para hippocampal gyrus, temporal pole- superior temporal gyrus, hippocampus, insula, lenticular nucleus-putamen, superior temporal gyrus, heschl gyrus, inferior frontal gyrus- triangular part, supramarginal gyrus, and supplementary motor area in the right hemisphere, as well as temporal pole- middle temporal gyrus, temporal pole- superior temporal gyrus, hippocampus, heschl gyrus, and supramarginal gyrus in the left hemisphere. The DC values for healthy participants and PNES patients in various regions of the brain network are represented in figure 3.
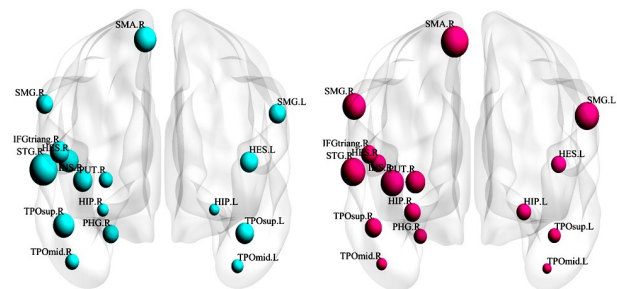

Figure 3. Mean values of degree of centrality for healthy participants (left) and PNES patients (right) in various brain network regions. SMR: supramarginal gyrus, IFG: inferior frontal gyrus, STG: superior temporal gyrus, HES: heschl gyrus, INS: insula, PUT: putamen, HIP: hippocampus, TPO: temporal pole, PHG: para hippocampal gyrus, and SMG: supramarginal gyrus.

Nodal efficiency (NF)

Our results showed that there are significant differences (P<0.04) in the NF values between the PNES patients and the healthy control participants in various regions of the brain, including temporal pole-middle temporal gyrus, fusiform gyrus, hippocampus, insula, lenticular nucleus-putamen, heschl gyrus, inferior frontal gyrus-triangular part, supramarginal gyrus, precuneus, inferior parietal- but supramarginal and angular gyri, and supplementary motor area in the right hemisphere, as well as temporal pole- middle temporal gyrus, temporal pole-superior temporal gyrus, hippocampus, insula, lenticular nucleus- putamen, heschl gyrus, supramarginal gyrus, inferior parietal, supramarginal and angular gyri in the left hemisphere. Figure 4 illustrates the mean values of NF for healthy individuals and PNES patient groups in various regions of the brain network.
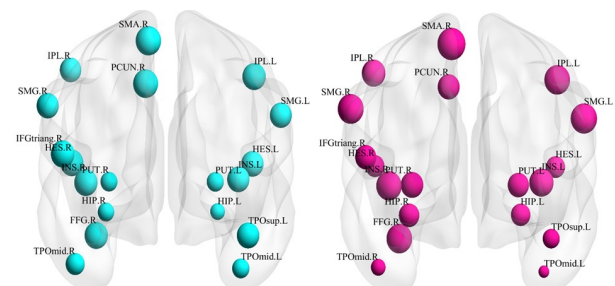

Figure 4. Mean values of nodal efficiency for healthy participants (left) and PNES patients (right) in various brain network regions. SMR: supramarginal gyrus, PCUN: posterior cingulate gyrus, IPL: inferior parietal, SMG: supramarginal gyrus, IFG: inferior frontal gyrus, HES: heschl gyrus, INS: insula, PUT: putamen, HIP: hippocampus, TPO: temporal pole, and FFG: fusiform gyrus.

Nodal local efficiency (NLF)

The results of comparing NLF between PNES patients with healthy control individuals showed that there are significant differences (P<0.03) in some of the brain network regions, including the insula, rolandic operculum, superior parietal gyrus in the right hemisphere, and the temporal pole-middle temporal gyrus, olfactory cortex, insula, inferior parietal-but supramarginal and angular gyri, precental gyrus, superior parietal gyrus, and supplementary motor area in the left hemisphere. Figure 5 shows the mean values of NLF for PNES patients and healthy individuals in various regions of the brain network.
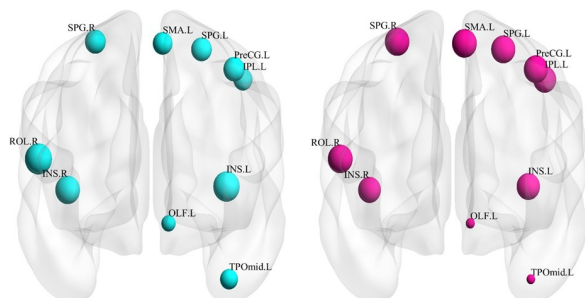

Figure 5. Mean values of nodal local efficiency for healthy participants (left) and PNES patients (right) in various brain network regions. SPG: superior parietal gyrus, SMA: supplementary motor area, PreCG: precental gyrus, IPL: inferior parietal, ROL: rolandic operculum, INS: insula, OLF: olfactory cortex, and TPO: temporal pole.

Nodal clustering coefficient (NCC)

NCC values were compared between PNES patients and healthy participants. The differences were significant (P <0.05) in several brain network regions, including the para hippocampal gyrus, fusiform gyrus, insula, rolandic operculum, supramarginal gyrus, and superior occipital gyrus in the right hemisphere, and temporal pole-middle temporal gyrus, olfactory cortex, insula, posterior cingulate gyrus, middle frontal gyrus, and supplementary motor area in the left hemisphere. The NCCs for PNES patients and healthy participants in various regions of the brain network are provided in figure 6.
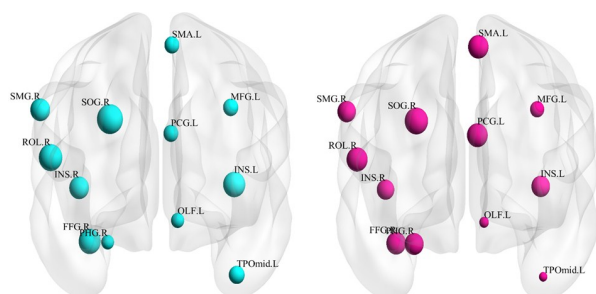

Figure 6. Mean values of nodal clustering coefficient for healthy participants (left) and PNES patients (right) in various brain network regions. SMA: supplementary motor area, SMG: supramarginal gyrus, SOG: superior occipital gyrus, PCG: posterior cingulate gyrus, ROL: rolandic operculum, INS: insula, FFG: fusiform gyrus, OLF: olfactory cortex, PHG: para hippocampal gyrus, and TPO: temporal pole.

Shortest pathway (Sh.P)

The PNES patients were compared with the healthy individuals regarding the Sh.P. The differences were significant in various brain regions (P<0.04), including the nodes of the temporal pole-middle temporal gyrus, para hippocampal gyrus, amygdala, hippocampus, lenticular nucleus-putamen, lenticular nucleus-pallidum, thalamus, caudate nucleus, median cingulate and paracingulate gyri in the right hemisphere, as well as, temporal pole- middle temporal gyrus, para hippocampal gyrus, amygdala, hippocampus, olfactory cortex, lenticular nucleus, putamen, lenticular nucleus, pallidum, thalamus, and caudate nucleus in the left hemisphere. Figure 7 shows the mean values of the Sh.P for PNES patients and healthy participants in various regions of the brain network.
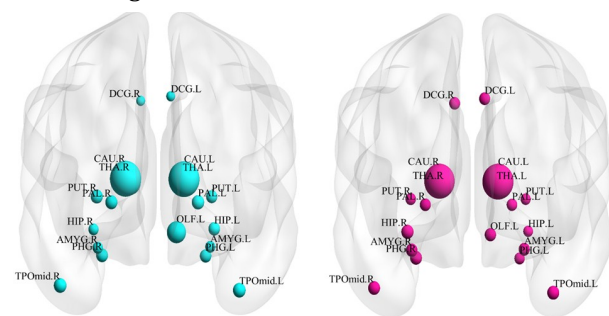

Figure 7. Mean values of shortest pathway for healthy participants (left) and PNES patients (right) in various brain network regions. DCG: paracingulate gyri, CAU: caudate nucleus, THA: thalamus, PUT: putamen, PAL: pallidum, HIP: hippocampus, OLF: olfactory cortex, AMYG: amygdala, PHG: para hippocampal gyrus, and TPO: temporal pole.

DISCUSSION

This study assessed the functional connectivity network of PNES patients in comparison with healthy individuals groups using graph theory analysis based on the fMRI images. We analyzed the brain networks with global and nodal (local) network parameters to determine the brain network differences among the investigated groups. Brain graph network modeling can illustrate the topological structure with quantitative parameters, and is one of the most important mathematical analysis tools [30,31].

Dienstag *et al.* [32] used rs-fMRI data to compare functional connectivity changes in brain networks for PNES patients and healthy participants. Their result showed disturbances between the medial temporal lobe, sensorimotor cortex, and ventral attention. Network connectivity was lower in the visual network of the PNES patients compared to healthy individuals. Their findings showed that PNES is related to changes in connectivity between areas related to memory processing, motor activity, and attention control. We also found that the brain alternations are significant in brain regions related to sensorimotor and attention activities. However, we

did not find substantial changes in the areas related to memory processing.

Li *et al.* [33] evaluated the alterations of regional and inter-regional network cerebral functions in PNES using rs-fMRI data to diagnose the functional connectivity and fractional amplitude of low-frequency fluctuations (fALFF). They reported that PNES patients had significantly higher values of fALFF in the dorsolateral prefrontal cortex, parietal cortices, and motor areas, as well as lower fALFF values in the triangular inferior frontal gyrus.

In another study by Amiri *et al.* [18], 23 PNES patients and 25 healthy individuals were assessed to obtain the alterations in whole brain functional connectivity with rs-fMRI. They expressed that the nodal degrees in the left orbital part of the left inferior frontal gyrus, right caudate, and right paracentral lobule was significantly higher in PNES patients (i.e., hyper-connectivity). On the other hand, a lower nodal degree (i.e., hypo-connectivity) was reported in several other brain regions, including the left and right insula, the right putamen, and the right middle occipital gyrus. In PNES patients, the brain areas with hypo-connectivity might be contributed in movement regulation (e.g., the putamen) and emotion processing (e.g., insula); however, the areas with hyper-connectivity may play a role in the inhibition of unwanted movements and cognitive processes (e.g., the caudate). Although we did not obtain the exact similar brain network alternations, our results were in agreement with the findings of the Amiri *et al.* study. For example, we also showed that NF values were lower in the left and right insula, as well as in right putamen of PNES patients. In general, we found that hypoactive regions in PNES patients were in similar areas involved in emotional procedures.

In the current study, changes in nodal properties have been observed in some areas related to patients' attention (insula, middle occipital gyrus, etc.). Insula is an important area of multisensory integration and mediates the interpretation of sensory information from the body, which is involved in emotion regulation, visceral sensory perception, and self-awareness [34]. Owing to the results, the DC, BC, and node efficiency in the insula in PNES patients are higher than in healthy individuals, indicating the insula's increasing role as a hub in receiving sensory information. This finding agrees with the results of previous studies showing the insula's role as an important hub for sensory information [35]. Also, the abnormal activity of the insula as a hub area causes the inability to inhibit behavioral responses to emotional stimuli. The nodal (local) efficiency of the insula in the PNES patient was lower than in the healthy participants in our study and also Amiri *et al.* [18], which means the insula has a lower effect on communication in PNES patients. The local clustering coefficient of the insula in the PNES patient group

was lower than the healthy individuals, indicating the insula's higher role in the brain networks of PNES patients. It can be expressed that the insula functions were changed in PNES patients such that the emotion is bolded in these patients.

The BC and local clustering coefficient in the PNES patients had significantly higher values compared to healthy control participants, indicating an increase in the role of the attention system in PNES patients. The value of the local clustering coefficient in the inferior frontal gyrus, orbital part, which is related to working memory and emotions, was lower in the PNES patients [36]. Based on our results, cingulate gyri, superior parietal gyrus, precentral gyrus, and supplementary motor area, which are the parts of the sensorimotor network, had incremental nodal quantity in the PNES patient. Higher values of the DC, NF, NLF, and NCC in the supplementary motor area of PNES patients, prove the idea that PNES can be related to altered movement and sensations [37]. During PNES episodes, sensorimotor and cognitive processes are affected and do not integrate properly, resulting in various unconscious behavioral patterns [38]. This study showed that hyperactivity in sensorimotor regions alters spontaneous and involuntary muscle movements and changes the functions of motor controllers in PNES patients.

CONCLUSION

The global brain network parameters calculated from fMRI images were similar between healthy participants and PNES patients. However, local brain network parameters showed many statistically significant differences in functional connectivity networks, including attentional, sensorimotor, default mode, executive control networks, and subcortical area. Our results agree with the hypoactivity in the functions of consciousness and motor control of PNES patients. In these patients, hyperactivity of emotion and motion control areas leads to reduce the role of the executive control areas.

or analyzed during the current study are available from the corresponding author on reasonable request.

Author contribution: MV is responsible for the study conception, design, acquisition of data, and finalizing of the manuscript. All the authors contributed to data analyzing and writing the manuscript draft. Furthermore, all the authors read and approved the final manuscript.

REFERENCES

1. Zhang J (2019) Basic neural units of the brain: neurons, synapses and action potential. arXiv preprint arXiv:190601703. E-book.
2. Uddin LQ (2021) Cognitive and behavioural flexibility: neural mechanisms and clinical considerations. *Nature Reviews Neuroscience, 22(3): 167–179*.
3. Proctor RW, and Van Zandt T (2018) Human factors in simple and complex systems. CRC press. E-book, 3rd Edition.
4. Welch JD, Kozareva V, Ferreira A, *et al.* (2019) Single-cell multiomic integration compares and contrasts features of brain cell identity. *Cell, 177(7): 1873–1887*.
5. Avena-Koenigsberger A, Misic B, Sporns O (2018) Communication dynamics in complex brain networks. *Nature Reviews Neuroscience, 19(1): 17–33*.
6. King JA, Frank GK, Thompson PM, Ehrlich S (2018) Structural neuroimaging of anorexia nervosa: future directions in the quest for mechanisms underlying dynamic alterations. *Biological Psychiatry, 83(3): 224–234*.
7. Perez DL, Nicholson TR, Asadi-Pooya AA, *et al.* (2021) Neuroimaging in functional neurological disorder: state of the field and research agenda. *NeuroImage: Clinical, 30:102623*.
8. Gonzalez-Astudillo J, Cattai T, Bassignana G, *et al.* (2021) Network-based brain–computer interfaces: principles and applications. *Journal of Neural Engineering, 18(1): 011001*.
9. Wang W, Mei M, Gao Y, *et al.* (2020) Changes of brain structural network connection in Parkinson's disease patients with mild cognitive dysfunction: a study based on diffusion tensor imaging. *Journal of Neurology, 267(4): 933–943*.
10. Kozlowska K, Chudleigh C, Cruz C, *et al.* (2018) Psychogenic non-epileptic seizures in children and adolescents: Part II–explanations to families, treatment, and group outcomes. *Clinical Child Psychology and Psychiatry, 23(1): 160–176*.
11. Goldstein LH and Mellers JD (2012) Recent developments in our understanding of the semiology and treatment of psychogenic nonepileptic seizures. *Current Neurology and Neuroscience Reports, 12(4): 436–444*.
12. Baslet G (2011) Psychogenic non-epileptic seizures: a model of their pathogenic mechanism. *Seizure, 20(1): 1–13*.
13. Cerasa A and Labate A (2018) The meaning of anxiety in patients with PNES. *Epilepsy & Behavior, 87: 248*.
14. Lanzillotti AI, Sarudiansky M, Lombardi NR, Korman GP. (2021) Updated review on the diagnosis and primary management of psychogenic nonepileptic seizure disorders. *Neuropsychiatric Disease and Treatment, 17: 1825-1838*.
15. Dörfel D, Gärtner A, Scheffel C. (2020) Resting state cortico-limbic functional connectivity and dispositional use of emotion regulation strategies: A replication and extension study. *Frontiers in Behavioral Neuroscience, 14: 128-141*.
16. Diez I, Ortiz-Terán L, Williams B, *et al.* (2019) Corticolimbic fast-tracking: enhanced multimodal integration in functional neurological disorder. *Journal of Neurology, Neurosurgery & Psychiatry, 90 (8): 929–938*.
17. Syan SK, Smith M, Frey BN, *et al.* (2018) Resting-state functional connectivity in individuals with bipolar disorder during clinical remission: a systematic review. *Journal of Psychiatry and Neuroscience, 43(5): 298–316*.
18. Amiri S, Mirbagheri MM, Asadi-Pooya AA, *et al.* (2021) Brain functional connectivity in individuals with psychogenic nonepileptic seizures (PNES): An application of graph theory. *Epilepsy & Behavior, 114: 107565*.
19. Allendorfer JB, Nenert R, Hernando KA, *et al.* (2019) FMRI response to acute psychological stress differentiates patients with psychogenic non-epileptic seizures from healthy controls–A biochemical and neuroimaging biomarker study. *NeuroImage: Clinical, 24: 101967*.
20. Zhai Q, Rahardjo H, Satyanaga A, *et al.* (2021) Estimation of wetting hydraulic conductivity function for unsaturated sandy soil. *Engineering Geology, 285: 106034*.
21. van der Kruijs SJ, Jagannathan SR, Bodde NM, *et al.* (2014) Resting-state networks and dissociation in psychogenic non-epileptic seizures. *Journal of Psychiatric Research, 54: 126–133*.
22. Meier B, Rothen N, Walter S. (2014) Developmental aspects of synaesthesia across the adult lifespan. *Frontiers in human neuroscience, 8: 129*.
23. Xia M, Wang J, He Y (2013) BrainNet Viewer: a network visualization tool for human brain connectomics. *PloS one, 8(7): e68910*.
24. Kocher M, Gleichgerrcht E, Nesland T, *et al.* (2015) Individual variability in the anatomical distribution of nodes participating in rich club structural networks. *Frontiers in Neural Circuits, 9(4): 1–7*.
25. van den Heuvel MP and Sporns O (2011) Rich-club organization of the human connectome. *Journal of Neuroscience, 31(44): 15775–86*.
26. Senden M, Deco G, De Reus MA, *et al.* (2014) Rich club organization supports a diverse set of functional network configurations. *NeuroImage, 96: 174–82*.
27. Januchowski-Hartley SR, Adams VM, Hermoso V (2018) The need for spatially explicit quantification of benefits in invasive-species management. *Conservation Biology, 32(2): 287–93*.
28. De Bona AA, Fonseca KVO, Rosa MO, *et al.* (2016) Analysis of public bus transportation of a Brazilian city based on the theory of complex networks using the P-space. *Mathematical Problems in Engineering, 2016: 3898762*.
29. Boccaletti S, Latora V, Moreno Y, *et al.* (2006) Complex networks: Structure and dynamics. Physics Reports, **424**(4–5): 175–308.
30. Fleischer V, Radetz A, Ciolac D, *et al.* (2019) Graph theoretical framework of brain networks in multiple sclerosis: a review of concepts. *Neuroscience, 403: 35–53*.
31. Sporns O (2022) Graph theory methods: applications in brain networks. Dialogues in clinical neuroscience.
32. Dienstag A, Ben-Naim S, Gilad M, *et al.* (2019) Memory and motor control in patients with psychogenic nonepileptic seizures. *Epilepsy & Behavior, 98: 279–284*.
33. Li R, Li Y, An D, *et al.* (2015) Altered regional activity and interregional functional connectivity in psychogenic non-epileptic seizures. *Scientific Reports, 5(1): 1–12*.
34. Pollatos O and Herbert BM (2018) Interoception: Definitions, dimensions, neural substrates. In: *Embodiment in Psychotherapy, 15 –27*.
35. Borsook D, Veggeberg R, Erpelding N, *et al.* (2016) The insula: a "hub of activity" in migraine. *The Neuroscientist, 22(6): 632–652*.
36. Buldú JM, Bajo R, Maestú F, *et al.* (2011) Reorganization of functional networks in mild cognitive impairment. *PLoS ONE, 6(5)*.
37. Brown RJ and Reuber M (2016) Towards an integrative theory of psychogenic non-epileptic seizures (PNES). *Clinical Psychology Review, 47: 55–70*.
38. Nayeri A, Rafla-Yuan E, Farber-Eger E, *et al.* (2017) Pre-existing psychiatric illness is associated with increased risk of recurrent Takotsubo cardiomyopathy. *Psychosomatics, 58(5): 527–532*.